

# Roles of Bridging Ligand Topology and Conformation in Controlling Exchange Interactions between Paramagnetic Molybdenum Fragments in Dinuclear and Trinuclear Complexes

Văn Ân Ung,<sup>†</sup> Alexander M. W. Cargill Thompson,<sup>†</sup> David A. Bardwell,<sup>†</sup> Dante Gatteschi,<sup>\*,‡</sup> John C. Jeffery,<sup>†</sup> Jon A. McCleverty,<sup>\*,†</sup> Federico Totti,<sup>‡</sup> and Michael D. Ward<sup>\*,†</sup>

School of Chemistry, University of Bristol, Cantock's Close, Bristol BS8 1TS, U.K., and Department of Chemistry, University of Florence, Via Maragliano 75/77, 50144 Florence, Italy

Received August 19, 1996<sup>⊗</sup>

The magnetic properties of two series of dinuclear complexes, and one trinuclear complex, have been examined as a function of the bridging pathway between the metal centers. The first series of dinuclear complexes is  $[\{\text{Mo}^{\text{V}}(\text{O})(\text{Tp}^*)\text{Cl}\}_2(\mu\text{-OO})]$ , where "OO" is  $[1,4\text{-O}(\text{C}_6\text{H}_4)_n\text{O}]^{2-}$  ( $n = 1, \mathbf{1}; n = 2, \mathbf{3}$ ),  $[4,4'\text{-O}(\text{C}_6\text{H}_3\text{-2-Me})_2\text{O}]^{2-}$  ( $\mathbf{4}$ ), or  $[1,3\text{-OC}_6\text{H}_4\text{O}]^{2-}$  ( $\mathbf{2}$ ) [ $\text{Tp}^* = \text{tris}(3,5\text{-dimethylpyrazolyl})\text{hydroborate}$ ]. The second series of dinuclear complexes is  $[\{\text{Mo}^{\text{I}}(\text{NO})(\text{Tp}^*)\text{Cl}\}_2(\mu\text{-NN})]$ , where "NN" is 4,4'-bipyridyl ( $\mathbf{5}$ ), 3,3'-dimethyl-4,4'-bipyridine ( $\mathbf{6}$ ), 3,8-phenanthroline ( $\mathbf{7}$ ), or 2,7-diazapyrene ( $\mathbf{8}$ ). The trinuclear complex is  $[\{\text{Mo}^{\text{V}}(\text{O})(\text{Tp}^*)\text{Cl}\}_3(1,3,5\text{-C}_6\text{H}_3\text{O}_3)]$  ( $\mathbf{9}$ ), whose crystal structure was determined  $[\mathbf{9} \cdot 5\text{CH}_2\text{Cl}_2: \text{C}_{56}\text{H}_{81}\text{B}_3\text{Cl}_{13}\text{Mo}_3\text{N}_{18}\text{O}_6$ ; monoclinic,  $P2_1/n$ ;  $a = 13.443$ ,  $b = 41.46(2)$ ,  $c = 14.314(6)$  Å;  $\beta = 93.21(3)^\circ$ ;  $V = 7995(5)$  Å<sup>3</sup>;  $Z = 4$ ;  $R_1 = 0.106$ ]. In these complexes, the sign and magnitude of the exchange coupling constant  $J$  is clearly related to both the topology and the conformation of the bridging ligand [where  $J$  is derived from  $H = -J\mathbf{S}_1 \cdot \mathbf{S}_2$  for  $\mathbf{1}\text{--}\mathbf{8}$  and  $H = -J(\mathbf{S}_1 \cdot \mathbf{S}_2 + \mathbf{S}_2 \cdot \mathbf{S}_3 + \mathbf{S}_1 \cdot \mathbf{S}_3)$  for  $\mathbf{9}$ ]. The values are as follows:  $\mathbf{1}$ ,  $-80$  cm<sup>-1</sup>;  $\mathbf{2}$ ,  $+9.8$  cm<sup>-1</sup>;  $\mathbf{3}$ ,  $-13.2$  cm<sup>-1</sup>;  $\mathbf{4}$ ,  $-2.8$  cm<sup>-1</sup>;  $\mathbf{5}$ ,  $-33$  cm<sup>-1</sup>;  $\mathbf{6}$ ,  $-3.5$  cm<sup>-1</sup>;  $\mathbf{7}$ ,  $-35.6$  cm<sup>-1</sup>;  $\mathbf{8}$ ,  $-35.0$  cm<sup>-1</sup>;  $\mathbf{9}$ ,  $+14.4$  cm<sup>-1</sup>. In particular the following holds: (1)  $J$  is negative (antiferromagnetic exchange) across the *para*-substituted bridges ligands of  $\mathbf{1}$  and  $\mathbf{3}\text{--}\mathbf{8}$  but positive (ferromagnetic exchange) across the *meta*-substituted bridging ligands of  $\mathbf{2}$  and  $\mathbf{9}$ . (2)  $J$  decreases in magnitude dramatically as the bridging ligand conformation changes from planar to twisted (compare  $\mathbf{3}$  and  $\mathbf{4}$ , or  $\mathbf{6}$  and  $\mathbf{8}$ ). These observations are consistent with a spin-polarization mechanism for the exchange interaction, propagated across the  $\pi$ -system of the bridging ligand by *via* overlap of bridging ligand  $p(\pi)$  orbitals with the  $d(\pi)$  magnetic orbitals of the metals. The EPR spectrum of  $\mathbf{9}$  is characteristic of a quartet species and shows weak  $\Delta m_s = 2$  and  $\Delta m_s = 3$  transitions at one-half and one-third, respectively, of the field strength of the principal  $\Delta m_s = 1$  component.

## Introduction

The ability to predict and control magnetic interactions between paramagnetic centers is of fundamental importance for the design and synthesis of new magnetic materials and discrete molecules with very high magnetic moments.<sup>1,2</sup> When the interacting centers are sufficiently close that the exchange interaction is mediated *via* direct orbital overlap, then the sign of the interaction depends on the relative symmetries of the two magnetic orbitals involved (the Goodenough–Kanamori rules),<sup>3</sup> and this principle has been exploited in controlling the magnetic properties of polynuclear coordination complexes.<sup>1,4</sup>

When the interacting paramagnetic centers are remote from one another, the interaction is more dependent on the orbitals of the bridging ligand, in two different ways: the superexchange and spin-polarization mechanisms. Even if the pure metal orbitals cannot directly overlap, mixing of these with the orbitals of the bridging ligand means that the magnetic orbitals may not be purely metal-centered but also have a significant ligand-based component, and in such cases direct overlap of the magnetic orbitals can still occur. This is the "superexchange" mechanism.

The spin-polarization mechanism arises from the molecular orbital model proposed by Longuet–Higgins for conjugated alternant hydrocarbons. This results in ferromagnetic coupling between two radicals which are separated by a *m*-phenylene bridge, because the two unpaired electrons reside in a pair of mutually orthogonal but degenerate SOMOs.<sup>5</sup> A consequence of this molecular orbital behavior is the well-known alternation of  $\alpha$  and  $\beta$  spin density induced on the intervening atoms (spin-polarization),<sup>6</sup> which has actually been detected and measured in some cases.<sup>7</sup> This simple principle has been the driving force

<sup>†</sup> University of Bristol.

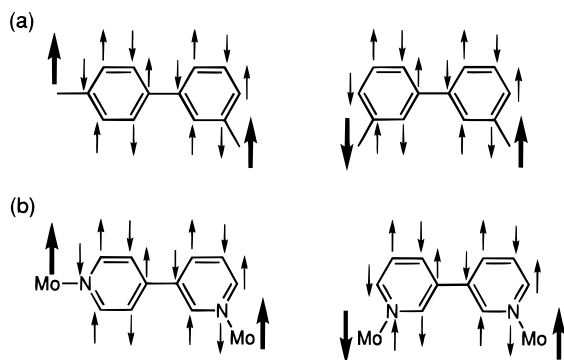
<sup>‡</sup> University of Florence.

<sup>⊗</sup> Abstract published in *Advance ACS Abstracts*, July 15, 1997.

- (1) (a) Kahn, O. *Molecular Magnetism*, VCH Publishers, Inc.: New York, 1993. (b) McCusker, J. K.; Schmitt, E. A.; Hendrickson, D. N. In *Magnetic Molecular Materials*; Gatteschi, D., Kahn, O., Miller, J. S., Palacio, F., Eds.; NATO ASI Series, Kluwer Academic Press: Dordrecht, The Netherlands, 1991; Vol. E198, p 297. (c) Kahn, O.; Pei, Y.; Journaux, Y. In *Inorganic Materials*; Bruce, D. W., O'Hare, D., Eds.; Wiley: Chichester, U.K., 1992; p 59. (d) Bushby, R. J.; Paillaud, J.-L. In *Introduction to Molecular Electronics*; Petty, M. C., Bryce, M. R., Bloor, D., Eds.; Edward Arnold: London, 1995; p 72. (e) Miller, J. S.; Epstein, A. J. *Angew. Chem., Int. Ed. Engl.* **1994**, *33*, 385.
- (2) Some recent examples: (a) De Munno, G.; Julve, M.; Lloret, F.; Faus, J.; Verdager, M.; Caneschi, A. *Inorg. Chem.* **1995**, *34*, 157. (b) Wemple, M. W.; Adams, D. M.; Hagen, K. S.; Folting, K.; Hendrickson, D. N.; Christou, G. *J. Chem. Soc., Chem. Commun.* **1995**, 1591. (c) Gordon-Wylie, S. W.; Bominaar, E. L.; Collins, T. J.; Workman, J. M.; Claus, B. L.; Patterson, R. E.; Williams, S. A.; Conklin, B. J.; Yee, G. T.; Weintraub, S. T. *Chem. Eur. J.* **1995**, *1*, 528. (d) Eppley, H. J.; Tsai, H.-L.; de Vries, N.; Folting, K.; Christou, G.; Hendrickson, D. N. *J. Am. Chem. Soc.* **1995**, *117*, 301.

- (3) (a) Kahn, O. *Struct. Bonding* **1987**, *68*, 89. (b) Goodenough, J. B. *Phys. Rev.* **1955**, *100*, 564. (c) Goodenough, J. B. *J. Phys. Chem. Solids* **1958**, *6*, 287. (d) Kanamori, J. *J. Phys. Chem. Solids* **1959**, *10*, 87. (e) Ginsberg, A. P. *Inorg. Chim. Acta Rev.* **1971**, *5*, 45.
- (4) (a) Gordon-Wylie, S. W.; Bominaar, E. L.; Collins, T. J.; Workman, J. M.; Claus, B. L.; Patterson, R. E.; Williams, S. A.; Conklin, B. J.; Yee, G. T.; Weintraub, S. T. *Chem. Eur. J.* **1995**, *1*, 528. (b) Nakatani, K.; Bergerat, P.; Codjovi, E.; Mathonière, C.; Pei, Y.; Kahn, O. *Inorg. Chem.* **1991**, *30*, 3977.
- (5) Longuet-Higgins, J. C. *J. Chem. Phys.* **1950**, *18*, 265.
- (6) (a) Karafiloglou, P. *J. Chem. Phys.* **1985**, *82*, 3728. (b) Ovchinnikov, A. A. *Theor. Chim. Acta* **1978**, *47*, 297.

**Scheme 1.** Effect of Bridging Pathway on the Sign of  $J$  in (a) Organic Diradicals with a Biphenyl Spacer<sup>10</sup> and (b) Dinuclear Molybdenum Complexes with a Bis(pyridyl) Bridging Ligand<sup>16 a</sup>



<sup>a</sup> The large arrows denote the unpaired spins; the small arrows denote the sign of the induced spin-polarization on the intervening atoms.

behind the preparation of numerous organic polyradicals exhibiting very high-spin ground states.<sup>1e,8</sup> Theoretical studies have evaluated the likely ability of other bridging groups to promote exchange interactions according to their topology,<sup>9</sup> and an interesting recent experimental result which nicely illustrates the spin-polarization effect is that a 3,4'-biphenyl bridge promotes ferromagnetic exchange between two unpaired spins whereas a 3,3'-biphenyl bridge promotes antiferromagnetic exchange (Scheme 1).<sup>10</sup> McConnell proposed that intermolecular interactions could also be rationalized by a spin-polarization mechanism,<sup>11</sup> and this has been used to rationalize the alignment of paramagnetic species in the solid state which can give rise to bulk ferromagnetism.<sup>12</sup>

The application of the spin-polarization effect to the design and synthesis of magnetic molecules containing metals as the paramagnetic centers has substantially lagged behind the development of organic ferromagnets, despite their obvious appeal. Advantages of inorganic over organic paramagnetic centers include higher spin density, improved chemical stability, and the possibility of reversible redox activity (for switching). Innumerable magnetically interesting coordination complexes are known,<sup>1a-d</sup> but examples in which the nature of the interaction between two or more remote metal centers can be controlled or predicted in advance according to the structure and conformation of the bridging ligand are very rare.<sup>13-16</sup> This is perhaps surprising considering the wealth of information that is available regarding the relationship between intermetallic

electronic interactions and the nature of the bridging ligand, which is manifested in the popular areas of mixed-valence complexes and "molecular wires".<sup>17</sup>

Oshio and co-workers have demonstrated that a ferromagnetic interaction occurs between two high-spin Fe(III) centers across a meta-substituted aromatic bridging ligand (based on deprotonated 1,3-dihydroxybenzene).<sup>13</sup> Likewise, Nogami and co-workers showed that the exchange interaction between vanadyl fragments across a pyrimidine bridge is ferromagnetic.<sup>14</sup> In both cases the ferromagnetism was ascribed to (i) the *meta* substitution pattern of the ligand and (ii)  $d(\pi)$ - $p(\pi)$  overlap between metal and ligand which allowed propagation of the exchange interaction by a simple spin-polarization mechanism involving the  $d(\pi)$  unpaired electrons on the metal ions and the  $p(\pi)$  electrons on the bridging ligand. In interesting contrast to these cases Hendrickson, Stucky, and co-workers showed that if the unpaired electrons of a metal fragment are in nonbonding orbitals which do not overlap with the  $\pi$ -system of the bridge, then such spin-polarization cannot occur and the exchange interaction may be antiferromagnetic even across a *meta*-substituted aromatic bridge.<sup>15</sup> *It follows that both the topology of the bridging ligand and the geometry of the metal-ligand overlap are crucial factors in the rational design of magnetically interesting polynuclear coordination complexes.*

We recently prepared a series of dinuclear complexes containing paramagnetic  $\{\text{Mo}(\text{NO})(\text{Tp}^*)\text{Cl}\}$  fragments attached to either end of a series of bis(pyridyl) bridging ligands and showed how the spin-polarization mechanism can be used to predict the sign of the exchange interaction according to the nature of the bridging ligand. In particular, we demonstrated for the first time that changing the length of the bridging pathway by one atom at a time results in an alternation of the sign of  $J$ , the exchange coupling constant (Scheme 1).<sup>16</sup>

It is apparent from these results that the same principles of molecular design that have been successfully applied to organic molecular magnets can also be applied to metal-based systems. This may allow a great deal of scope for modifying the exchange interaction by changing the conformational and topological properties of the bridging pathway linking the interacting spins. We were accordingly interested in the following questions.

Can the behavior we observed for  $\{\text{Mo}(\text{NO})(\text{Tp}^*)\text{Cl}\}$  fragments attached to pyridyl bridging ligands be extended to other metal fragments/bridging ligands?

Given that all simple spin-polarization models involve the  $\pi$ -electrons of the organic bridge, can the exchange interaction be modulated by imposing conformational changes on the bridging ligand which would decouple the  $\pi$ -system?

Can the simple predictive model be extended to higher nuclearity complexes?

We describe here the magnetic properties of a series of dinuclear and trinuclear complexes based on  $\{\text{Mo}(\text{NO})(\text{Tp}^*)\text{Cl}\}$  and  $\{\text{Mo}(\text{O})(\text{Tp}^*)\text{Cl}\}^+$  fragments (Chart 1) which illuminate these questions.

## Experimental Section

Complexes **1-4**<sup>18</sup> and **5** and **6**,<sup>19</sup> the ligands 3,8-phenanthroline<sup>20</sup> and 2,7-diazapyrene,<sup>21</sup> and  $[\text{Mo}(\text{NO})(\text{Tp}^*)\text{Cl}_2]$ <sup>22</sup> were all prepared according to the previously published methods.

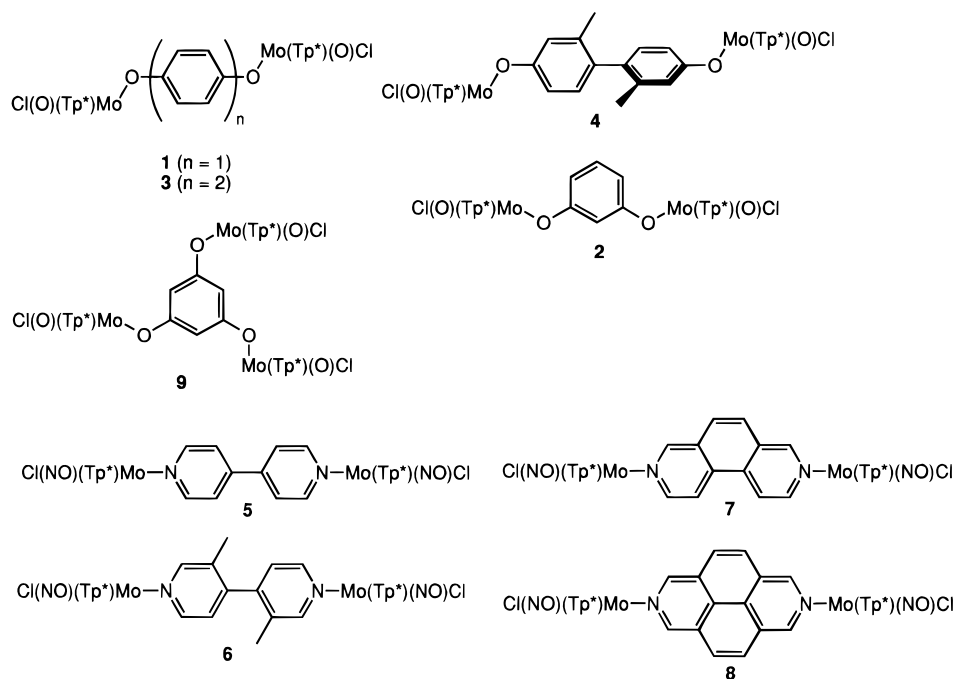
**Preparation of 7 and 8.** These were prepared by exactly the same method used to prepare **5** and **6**:<sup>19</sup> *viz.* reaction of the appropriate bridging ligand with >2 equiv of  $[\text{Mo}(\text{NO})(\text{Tp}^*)\text{Cl}_2]$  under  $\text{N}_2$  in dry toluene at reflux in the presence of  $\text{Et}_3\text{N}$ , followed by chromatographic

- (7) (a) Okamoto, M.; Teki, Y.; Takui, T.; Kinoshita, T.; Itoh, K. *Chem. Phys. Lett.* **1990**, *173*, 265. (b) Takui, T.; Kita, S.; Ichikawa, S.; Teki, Y.; Kinoshita, T.; Itoh, K. *Mol. Cryst. Liq. Cryst.* **1989**, *176*, 67.
- (8) (a) Mataga, N. *Theor. Chim. Acta* **1968**, *10*, 372. (b) Iwamura, H. *Pure Appl. Chem.* **1993**, *65*, 57. (c) Rajca, S. *Chem. Rev.* **1994**, *94*, 871. (d) Iwamura, H. *Mol. Cryst. Liq. Cryst.* **1993**, *232*, 233. (e) Buchachenko, A. *Mol. Cryst. Liq. Cryst.* **1989**, *176*, 67. (f) Rajca, S.; Rajca, A. *J. Am. Chem. Soc.* **1995**, *117*, 9172. (g) Yoshizawa, K.; Hoffman, R. *Chem. Eur. J.* **1995**, *1*, 403. (h) Iwamura, H.; Koga, N. *Acc. Chem. Res.* **1993**, *26*, 346. (i) Dougherty, D. A. *Acc. Chem. Res.* **1991**, *24*, 88.
- (9) (a) Lahti, P. M.; Ichimura, A. S. *J. Org. Chem.* **1991**, *56*, 3030. (b) Li, S.; Ma, J.; Jiang, Y. *Chem. Phys. Lett.* **1995**, *246*, 221.
- (10) (a) Rajca, A.; Rajca, S. *J. Am. Chem. Soc.* **1996**, *118*, 8121. (b) Minato, M.; Lahti, P. M.; van Willigen, H. *J. Am. Chem. Soc.* **1993**, *115*, 4532.
- (11) McConnell, H. M. *J. Chem. Phys.* **1963**, *39*, 1910.
- (12) Yoshizawa, K.; Hoffman, R. *J. Am. Chem. Soc.* **1995**, *117*, 6921.
- (13) (a) Oshio, H. *J. Chem. Soc., Chem. Commun.* **1991**, 240. (b) Oshio, H.; Ichida, H. *J. Phys. Chem.* **1995**, *99*, 3294.
- (14) Mitsubori, S.; Ishida, T.; Nogami, T.; Iwamura, H. *Chem. Lett.* **1994**, 285.
- (15) (a) Francesconi, L. C.; Corbin, D. R.; Hendrickson, D. N.; Stucky, G. D. *Inorg. Chem.* **1979**, *18*, 3074. (b) Fieselman, B. F.; Hendrickson, D. F.; Stucky, G. D. *Inorg. Chem.* **1978**, *17*, 1841.

- (16) Cargill Thompson, A. M. W.; Gatteschi, D.; McCleverty, J. A.; Navas, J. A.; Rentschler, E.; Ward, M. D. *Inorg. Chem.* **1996**, *35*, 2701.

- (17) Ward, M. D. *Chem. Soc. Rev.* **1995**, *24*, 121.

## Chart 1



purification (silica;  $\text{CH}_2\text{Cl}_2/\text{thf}$ , 99:1 v/v). The yields were 30–40% in both cases. Both complexes gave strong molecular ions at the correct position in their FAB mass spectra ( $m/z = 1098$  for **7** and  $1122$  for **8**), whose isotopic patterns were appropriate for the formulations. Correct elemental analyses ( $\pm 0.4\%$  for C, H, N) were also obtained. The EPR spectra of **7** and **8** also confirmed their dinuclear character, showing typical spectra with all of the features apparent for coupling to two molybdenum nuclei being apparent and a hyperfine separation between signal components of *ca.* 25 G.<sup>19,23</sup>

**Preparation of 9.** A mixture of 1,3,5-trihydroxybenzene (0.33 mmol),  $[\text{Mo}(\text{O})(\text{Tp}^*)\text{Cl}_2]$  (1 mmol), and dry  $\text{Et}_3\text{N}$  (few drops, excess) in dry toluene was heated to reflux under  $\text{N}_2$  while stirring. After all of the  $[\text{Mo}(\text{O})(\text{Tp}^*)\text{Cl}_2]$  was consumed (checked by thin-layer chromatography with silica/ $\text{CH}_2\text{Cl}_2$ ) the mixture was cooled, filtered to remove  $[\text{Et}_3\text{NH}]\text{Cl}$ , and evaporated to dryness. The residue was purified by column chromatography (silica,  $\text{CH}_2\text{Cl}_2$ ); the desired product was the first major purple band to elute and was obtained in 58% yield. FABMS:  $m/z = 1457$  ( $\text{M}^+$ ). Anal. Found (calcd): C, 42.2 (42.0); H, 4.9 (4.7); N, 17.0 (17.3). IR spectrum (KBr disk):  $\nu(\text{B-H}) = 2547 \text{ cm}^{-1}$ ;  $\nu(\text{Mo=O}) 949 \text{ cm}^{-1}$ . Other dinuclear and trinuclear products from this reaction were also characterized and will be described separately.

**Crystal Structure of  $9 \cdot 5\text{CH}_2\text{Cl}_2$ .** Purple crystals of  $9 \cdot 5\text{CH}_2\text{Cl}_2$  were grown by diffusion of ether into a concentrated  $\text{CH}_2\text{Cl}_2$  solution of **9**. The crystals were thin plates; that selected had dimensions  $0.3 \times 0.2 \times 0.05 \text{ mm}^3$  and was rapidly coated with paraffin oil and mounted on a brass pin on the diffractometer under a stream of cold  $\text{N}_2$ . Crystallographic data are summarized in Table 1. A Siemens SMART diffractometer (three circles and a CCD-type area detector) was used to collect 36 913 reflections ( $2\theta_{\text{max}} = 50^\circ$ ) at  $-100^\circ\text{C}$ , which after

**Table 1.** Crystallographic Data for  $9 \cdot 5\text{CH}_2\text{Cl}_2$

chem formula	$\text{C}_{56}\text{H}_{81}\text{B}_3\text{Cl}_{13}\text{Mo}_3\text{N}_{18}\text{O}_6$
fw	1883.49
space group	$P2_1/n$
$a$ , Å	13.443(4)
$b$ , Å	41.62(2)
$c$ , Å	14.314(6)
$\beta$ , deg	93.21(3)
$V$ , Å <sup>3</sup>	7995(5)
$Z$	4
$\rho_{\text{calc}}$ , g $\text{cm}^{-3}$	1.565
$\mu(\text{Mo K}\alpha)$ , $\text{mm}^{-1}$	0.954
$T$ , K	173(2)
$\lambda$ , Å	0.710 73
$R_1$ , $wR_2^{a,b}$	0.106, 0.270

<sup>a</sup> Structure was refined on  $F_o^2$  using all data; the value of  $R_1$  is given for comparison with older refinements based on  $F_o$  with a typical threshold of  $F \geq 4\sigma(F)$ . <sup>b</sup>  $wR_2 = [\sum[w(F_o^2 - F_c^2)^2]/\sum w(F_o^2)^2]^{1/2}$ , where  $w^{-1} = [\sigma^2(F_o^2) + (aP)^2 + bP]$  and  $P = [\max(F_o^2, 0) + 2F_c^2]/3$  ( $a = 0.1073$ ,  $b = 35.83$ ).

merging afforded 13 929 unique data ( $R_{\text{int}} = 0.116$ ). An empirical absorption correction, and corrections for Lorentz and polarization effects, were applied. The structure was solved by direct methods and refined by the full-matrix least-squares method on all  $F^2$  data using the SHELX suite of programs.<sup>24</sup> Refinement of 911 parameters with 121 restraints converged at  $R_1 = 0.1064$  for selected data with  $I > 2\sigma(I)$ ;  $wR_2 = 0.2703$  (all data). All non-hydrogen atoms were refined with anisotropic thermal parameters; hydrogen atoms were included in calculated positions and refined isotropically. The asymmetric unit contains one trinuclear complex and five independent molecules of  $\text{CH}_2\text{Cl}_2$ , to which weak restraints were applied to keep the C–Cl bond lengths stable during refinement. One  $\text{CH}_2\text{Cl}_2$  molecule was disordered over two positions and refined with site occupancies of 0.55/0.45. The large number of lattice solvent molecules posed problems of partial decomposition during transfer from the mother liquor to the diffractometer and also some disorder. Together with the small crystal size this resulted in a relatively poor refinement ( $R_1 = 10.6\%$ ); however the structure of the complex is clear and the precision of the structural parameters reasonable.

Apparatus used for electrochemical<sup>19,23</sup> and magnetic<sup>16</sup> measurements has been described earlier. Magnetic susceptibilities were recorded

- (18) Ung, V. A.; Bardwell, D. A.; Jeffery, J. C.; Maher, J. P.; McCleverty, J. A.; Ward, M. D.; Williamson, A. *Inorg. Chem.* **1996**, *35*, 5290.  
 (19) Das, A.; Maher, J. P.; McCleverty, J. A.; Navas, J. A.; Ward, M. D. *J. Chem. Soc., Dalton Trans.* **1993**, 681.  
 (20) Bartrop, J. A.; Jackson, A. C. *J. Chem. Soc., Perkin Trans. 2* **1984**, 367.  
 (21) Stang, P. J.; Cao, D. H.; Saito, S.; Arif, A. M. *J. Am. Chem. Soc.* **1995**, *117*, 6273.  
 (22) (a) Jones, C. J.; McCleverty, J. A.; Reynolds, S. J.; Smith, C. F. *Inorg. Synth.* **1985**, *23*, 4. (b) Trofimenko, S. *Inorg. Chem.* **1969**, *8*, 2675. (c) Drane, A. S.; McCleverty, J. A. *Polyhedron* **1983**, *2*, 53.  
 (23) (a) Das, A.; Jeffery, J. C.; Maher, J. P.; McCleverty, J. A.; Schatz, E.; Ward, M. D.; Wollermann, G. *Inorg. Chem.* **1993**, *32*, 2145. (b) Amoroso, A. J.; Cargill Thompson, A. M. W.; Maher, J. P.; McCleverty, J. A.; Ward, M. D. *Inorg. Chem.* **1995**, *34*, 4828.

- (24) SHELXTL program system, version 5.03, Siemens Analytical X-ray Instruments, Madison, WI, 1995.

**Table 2.** Summary of Magnetic Exchange and Electrochemical Interactions in the Complexes

complex	magnetic data			$\Delta E_{1/2}$ , mV	
	$J$ , cm <sup>-1</sup>	$g$	TIP		
			( $\times 10^4$ )	Mo(V)/Mo(VI) <sup>a</sup>	Mo(I)/Mo(0) <sup>b</sup>
<b>1</b>	-80 <sup>c</sup>	1.90	14	990 <sup>e</sup>	
<b>2</b>	+9.8 <sup>c</sup>	1.99	0.5	n/a <sup>c</sup>	
<b>3</b>	-13.2 <sup>c</sup>	1.90	0.5	480 <sup>e</sup>	
<b>4</b>	-2.8 <sup>c</sup>	1.99	0.5	230 <sup>e</sup>	
<b>5</b>	-33 <sup>d</sup>				765 <sup>f</sup>
<b>6</b>	-3.5 <sup>c</sup>	1.83	8		380 <sup>f</sup>
<b>7</b>	-35.6 <sup>c</sup>	1.79	3.5		790 <sup>e</sup>
<b>8</b>	-35.0 <sup>c</sup>	1.84	2.6		730 <sup>e</sup>
<b>9</b>	+14.4 <sup>c</sup>	1.92	2.8	n/a <sup>c</sup>	

<sup>a</sup>  $\Delta E_{1/2}$  is the separation between the Mo(V)/Mo(VI) couples for the oxo-Mo(V) complexes, except for **2** and **9** which show just a single irreversible oxidation. <sup>b</sup>  $\Delta E_{1/2}$  is the separation between the Mo(I)/Mo(0) couples for the nitrosyl-Mo(I) complexes. <sup>c</sup> This work. <sup>d</sup> From ref 16. <sup>e</sup> From ref 18. <sup>f</sup> From ref 19.

over the range 1.2–230 K and analyzed by using a standard least-squares fitting procedure with spin Hamiltonians of the form  $H = -J\mathbf{S}_1 \cdot \mathbf{S}_2$  for dinuclear complexes **1–8**, and  $H = -J(\mathbf{S}_1 \cdot \mathbf{S}_2 + \mathbf{S}_2 \cdot \mathbf{S}_3 + \mathbf{S}_1 \cdot \mathbf{S}_3)$  for trinuclear complex **9**, with positive  $J$  indicating ferromagnetism and negative  $J$  indicating antiferromagnetism. The singlet–triplet gap for **1–8** is therefore  $J$ , and the quartet–doublet gap for **9** is  $3/2J$ . The values of  $J$  together with the values of  $g$  and temperature-independent paramagnetism (TIP) used in the fitting are summarized in Table 2. All of the dinuclear complexes obey the Bleaney–Bowers equation.<sup>1a</sup>

X-band EPR spectra were recorded with a Bruker ESP-300E spectrometer. The frozen glass spectrum of **9** (CH<sub>2</sub>Cl<sub>2</sub>/thf, 2:1) was recorded at 77 K under the following conditions: microwave frequency, 9.439 GHz; microwave power, 20 mW; modulation amplitude, 2 G. The  $\Delta m_s = 3$  transition was not immediately apparent but emerged after several hundred accumulations were averaged at high receiver gain.

## Results and Discussion

**Magnetic Properties of Dinuclear Complexes 1–4.** The dinuclear complexes **1–4**, containing {Mo<sup>V</sup>(O)(Tp\*)Cl}<sup>+</sup> fragments attached to either end of bis-phenolic bridging ligands of varying lengths, substitution pattern, and conformation, were prepared originally in order to evaluate electrochemical interactions across the different bridging ligands.<sup>18</sup> The EPR spectra of the complexes showed evidence for exchange (e.g.  $\Delta m_s = 2$  transitions were apparent at 77 K) which has prompted us to measure their magnetic properties. Their magnetic susceptibilities were recorded at temperatures down to 1.2 K. The values of  $J$  derived from these measurements are -80, +9.8, -13.2, and -2.8 cm<sup>-1</sup> for **1–4**, respectively (Table 2).

Complex **2** (with the *meta*-substituted bridge) is the only one displaying ferromagnetic exchange—all of the others are antiferromagnetic. The change in sign of  $J$  between **1** and **2** as the bridging pathway changes in length by one atom is in accord with the prediction of the spin-polarization mechanism that the sign of  $J$  should alternate as the number of atoms in the bridging pathway increases.<sup>16</sup> Other workers have likewise observed ferromagnetic exchange between paramagnetic metal centers across *meta*-substituted bridging ligands.<sup>13,14</sup> Comparison of **1** and **3** shows how the magnetic interaction decreases in magnitude (from -80 to -13.2 cm<sup>-1</sup>) as the bridging ligand lengthens and becomes nonplanar. A molecular mechanics calculation on **3** suggested a dihedral twist angle of about 37° between the two halves of the bridging ligand,<sup>18</sup> which is typical for a biphenyl-type bridge.<sup>25</sup> Complex **4**, with sterically

hindering methyl groups in the bridging ligand, has a (computed) dihedral twist of 87°. The increased dihedral twist between **3** and **4** results in a dramatic decrease in the antiferromagnetic coupling, with  $J$  diminishing from -13.2 to -2.8 cm<sup>-1</sup>. Since the increased twist of **4** will decouple the  $\pi$ -overlap between the two halves of the complex, this confirms that the magnetic interaction in these complexes is propagated principally *via* the  $\pi$ -system. The residual coupling of -2.8 cm<sup>-1</sup> in **4** could arise because the two phenyl rings are not exactly perpendicular in the solid state; a weak coupling through the  $\sigma$ -bonding network is also possible, as has long been known for saturated nitroxide diradicals.<sup>26</sup> Although the dipolar interaction between the unpaired spins is sensitive to the relative orientations of the two metal centers,<sup>27</sup> over this distance the dipolar interaction is likely to be very weak and the dependence of  $J$  on ligand conformation must be predominantly due to decoupling of the  $\pi$ -system in **4**.

The exchange interactions in these complexes are remarkably large (e.g. -80 cm<sup>-1</sup> for **1**) considering the presence of formally sp<sup>3</sup>-hybridized phenolate oxygen atoms in the bridging pathway, which would interrupt the conjugation in the bridge. This suggests that in fact the hybridization of the phenolate oxygen atoms is sp<sup>2</sup>, with the p<sub>z</sub> orbital providing the  $\pi$ -overlap between the Mo center and the aromatic bridge which is necessary for propagation of the spin-polarization. Related behavior was demonstrated in dinuclear molybdenum complexes of *ortho*, *meta* and *para* [C<sub>6</sub>H<sub>4</sub>(NH<sub>2</sub>)<sub>2</sub>]<sup>2-</sup> in which the trigonal hybridization of the amide N atoms promoted strong interactions between metal centers by providing a fully conjugated bridging pathway.<sup>28</sup> The crystal structures of **1** and **2** show that the angles at the phenolate oxygen atoms are *ca.* 135°,<sup>18</sup> which is nearer the value expected for trigonal than tetrahedral hybridization but is still substantially larger than both for obvious steric reasons.

**Magnetic Properties of Dinuclear Complexes 5–8.** In our earlier work on the magnetic properties of dinuclear complexes containing {Mo(NO)(Tp\*)Cl} fragments attached to bis(pyridyl) bridging ligands, it was apparent that the torsion angle between the two pyridyl rings was modulating the exchange interaction.<sup>16</sup> Thus, in the series of complexes with 3,3'-bipyridyl, 3,4'-bipyridyl, and 4,4'-bipyridyl, the signs of  $J$  alternated as expected but the magnitudes of  $J$  were affected unpredictably by the fact that in each complex the bridging ligand conformation (twist angle) was different for steric reasons.<sup>16</sup> To probe this further, we have measured the magnetic properties of a series of dinuclear complexes **5–8**, based on a 4,4'-bipyridyl-type linkage in which the dihedral twist of the bridge is varied. In complex **5** this angle was computed to be 26°, in **6** it is 90° (cf. complex **4**), and in **7** and **8** the rigidly constrained bridging ligands are essentially planar.

The values of  $J$  calculated from variable-temperature magnetic susceptibility measurements are summarized in Table 2. We knew from our previous work that complex **5** was strongly antiferromagnetically coupled with  $J = -33$  cm<sup>-1</sup>.<sup>16</sup> In **6** however, the near-orthogonality of the two pyridyl rings in the bridging ligand results in a substantial decrease in the magnitude of  $J$ , to just -3.5 cm<sup>-1</sup>. As with **4**, the residual exchange interaction may be ascribed to a slight degree of  $\pi$ -overlap remaining if the pyridyl rings are not exactly orthogonal and/or an interaction through the  $\sigma$ -bonding network (an exchange interaction has been detected by EPR spectroscopy

(26) Brière, R.; Dupeyre, R.-M.; Lemaire, H.; Morat, C.; Rassat, A.; Rey, P. *Bull. Soc. Chim. Fr.* **1965**, *11*, 3290.

(27) Chow, C. D.; Willett, R. D. *J. Chem. Phys.* **1973**, *59*, 5903.

(28) Włodarczyk, A.; Maher, J. P.; McCleverty, J. A.; Ward, M. D. *J. Chem. Soc., Chem. Commun.* **1995**, 2397.

between two  $\{\text{Mo}(\text{NO})(\text{Tp}^*)\text{Cl}(\text{pyridyl})\}$  centers across a  $\text{CH}_2\text{-CH}_2$  bridge).<sup>29</sup>

In **7** and **8** by contrast the bridging ligands are constrained to be essentially planar, and in these the values of  $J$  are  $-35.6$  and  $-35.0 \text{ cm}^{-1}$ , respectively, which are similar both to each other and slightly greater than the value of  $-33 \text{ cm}^{-1}$  observed for **5**. 3,8-Phenanthroline and 2,7-diazapyrene are of course not just "conformational isomers" of 4,4'-bipyridine: They are also substantially different electronically because of the increased conjugation and the different energies of their orbitals compared to 4,4'-bipyridine, which could influence the exchange interaction independently of conformational effects. However if this were significant, we would expect **7** and **8** to have significantly different values of  $J$ , which they do not: This observation, together with the marked difference between **5** and **6** where only conformational effects are significant, leads us to believe that the slightly increased exchange interactions in **7** and **8** compared to **5**, and the substantially reduced interaction in **6**, are mainly due to the conformation of the bridging ligand.

**Discussion of Results in the Two Sets of Dinuclear Complexes.** The two sets of complexes described above show very similar behavior. This may in part be due to the fact that the simple principles which underly these results are universal and will apply equally well to a wide variety of such systems. It is also worth pointing out, however, that despite their different oxidation states both the  $\{\text{Mo}(\text{NO})(\text{Tp}^*)\text{Cl}(\text{pyridyl})\}$  and  $\{\text{Mo}(\text{O})(\text{Tp}^*)\text{Cl}(\text{phenolate})\}$  fragments have the same magnetic orbital (SOMO). In the former case, the Mo center is formally in oxidation state +1 ( $d^5$  configuration). If the Mo-NO axis is taken as the  $z$ -axis, the metal  $d_{xz}$  and  $d_{yz}$  orbitals are lowered by interaction with the two empty  $\pi^*$  orbitals of the nitrosyl ligand, whereas the  $d_{xy}$  is not; the configuration is therefore  $(d_{xz})^2(d_{yz})^2(d_{xy})^1$ .<sup>30</sup> In the latter case, the Mo center is in oxidation state +5 ( $d^1$  configuration). If the Mo=O axis is taken as the  $z$ -axis, the metal  $d_{xz}$  and  $d_{yz}$  orbitals are raised by interaction with the filled  $p_x$  and  $p_y$  orbitals of the oxo ligand, whereas the  $d_{xy}$  is not; the configuration is therefore  $(d_{xy})^1(d_{xz})^0(d_{yz})^0$  with  $d_{xy}$  again being the SOMO.<sup>18</sup> In both types of complex the bridging ligand terminus (pyridyl or phenolate, respectively) approaches the metal along the  $x$ -axis, and therefore the spatial relationship between the  $\pi$ -system of this ligand and the SOMO will be similar in each case. In **5**–**8** the SOMO overlaps directly with the  $\pi$ -system of the pyridyl ligand, which allows the unpaired spin on the metal to induce a polarization of spin on the ligand atoms. In **1**–**4** it is necessary to assume that an oxygen  $p$ -orbital provides the bridge between the metal  $d(\pi)$  and ligand  $p(\pi)$  orbitals, but there is reasonable evidence for this as mentioned above. In both types of complex therefore the exchange interaction is transmitted principally through the  $\pi$ -system of the bridging ligand, *via* overlap of the  $\pi$ -symmetry SOMOs (Mo- $d_{xy}$ ) with the  $\pi$ -systems of the bridging ligands.

A dependence of  $J$  on the conformation of the bridging ligand is therefore to be expected but it is nonetheless striking, and the measurements described in this paper are the first concrete examples of such an effect. It is interesting to compare this with the extent to which electrochemical interactions are also modified by bridging ligand conformation. The relevant electrochemical data are included in Table 2. In the oxo-Mo(V) complexes, a change in the (computed) torsion angle

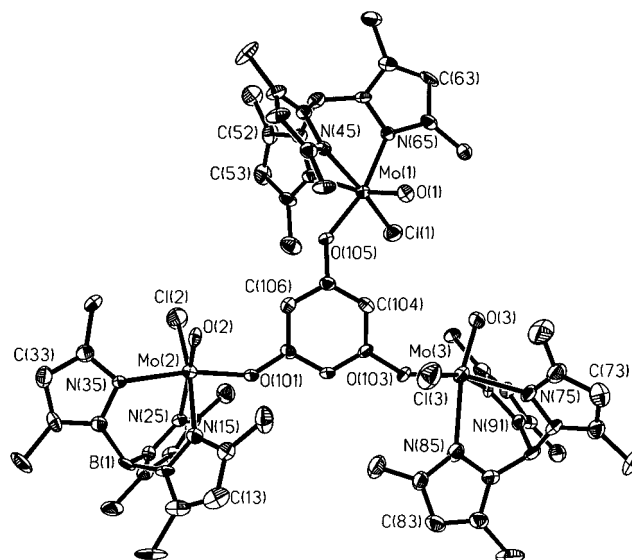


**Figure 1.** ORTEP plot of the complex unit of **9**·5( $\text{CH}_2\text{Cl}_2$ ), showing thermal ellipsoids at the 40% probability level.

from  $37^\circ$  (**3**) to near-orthogonal (**4**) results in a decrease in the magnitude of  $J$  by *ca.* 80%. In the same pair of complexes, the separation between the two Mo(V)/Mo(VI) redox potentials drops from 480 to 230 mV, a decrease of just over 50%. For the nitrosyl-Mo(I) complexes, the change from planar (**7**, **8**) to near-orthogonal (**6**) results in a decrease of about 90% in the magnitude of  $J$  but only about 50% in the separation between the two Mo(I)/Mo(0) couples. Although both electrochemical and magnetic properties are sensitive to the nature of the  $\pi$ -system linking the metal centers, they clearly do not depend upon it in the same way: the ability of a bridging ligand to delocalize charge (electrochemical interaction) is not directly related to its ability to transmit magnetic interactions by spin-polarization.

The sensitivity of the exchange interactions in these complexes to the conformation of the bridging ligand is encouraging from the point of view of developing viable switching mechanisms to control the properties of molecular materials. Many bridging ligands are known whose conformation can be modified by allosteric<sup>31</sup> or electrochemical<sup>32</sup> methods; use of such ligands in the preparation of multimetallic arrays of paramagnetic centers would allow the possibility of the magnetic properties of the array to be switched between two very different states.

**Synthesis and Properties of Trinuclear Complex 9.** Following the results from both series of dinuclear complexes, we were interested to extend our studies to higher nuclearity systems. We have previously shown by EPR spectroscopic measurements that exchange interactions between three and four  $\{\text{Mo}(\text{NO})(\text{Tp}^*)\text{Cl}\}$  centers can occur across bridging ligands which contain several pyridyl fragments pendant from a central aromatic core.<sup>23b</sup> However, over the large metal-metal distances involved in these complexes the interactions are likely to be too weak to be measured accurately by susceptibility studies. We therefore sought a multinucleating bridging ligand which would allow assembly of several metal centers with metal-metal pathways short enough to give measurable exchange interactions and decided on 1,3,5-trihy-

(29) McWhinnie, S. L. W.; Jones, C. J.; McCleverty, J. A.; Collison, D.; Mabbs, F. E. *J. Chem. Soc., Chem. Commun.* **1990**, 940.

(30) McWhinnie, S. L. W.; Thomas, J. A.; Hamor, T. A.; Jones, C. J.; McCleverty, J. A.; Collison, D.; Mabbs, F. E.; Harding, C. J.; Yellowlees, L. J.; Hutchings, M. G. *Inorg. Chem.* **1996**, *35*, 760.

(31) (a) Gourdon, A. *New J. Chem.* **1992**, *16*, 953. (b) Beer, P. D.; Chan, Z.; Grieve, A.; Haggitt, J. *J. Chem. Soc., Chem. Commun.* **1994**, 2413.

(32) (a) Joulié, L. F.; Schatz, E.; Ward, M. D.; Weber, F.; Yellowlees, L. J. *J. Chem. Soc., Dalton Trans.* **1994**, 799. (b) Metcalfe, R. A.; Dodsworth, E. S.; Lever, A. B. P.; Pietro, W. J.; Stufkens, D. *J. Inorg. Chem.* **1993**, *32*, 3581.

**Table 3.** Selected Bond Lengths (Å) and Angles (deg) for **9**·5CH<sub>2</sub>Cl<sub>2</sub>

Mo(1)–O(1)	1.733(8)	Mo(2)–O(2)	1.774(7)	Mo(3)–O(3)	1.703(8)
Mo(1)–O(105)	1.923(7)	Mo(2)–O(101)	1.936(7)	Mo(3)–O(103)	1.923(8)
Mo(1)–Cl(1)	2.345(3)	Mo(2)–Cl(2)	2.284(4)	Mo(3)–Cl(3)	2.325(4)
Mo(1)–N(45)	2.160(9)	Mo(2)–N(25)	2.293(9)	Mo(3)–N(95)	2.155(10)
Mo(1)–N(65)	2.200(9)	Mo(2)–N(15)	2.187(9)	Mo(3)–N(75)	2.197(10)
Mo(1)–N(55)	2.320(10)	Mo(2)–N(35)	2.148(9)	Mo(3)–N(85)	2.332(11)
O(1)–Mo(1)–O(105)	103.2(4)	O(2)–Mo(2)–O(101)	99.1(3)	O(3)–Mo(3)–O(103)	103.3(4)
O(1)–Mo(1)–N(45)	93.6(4)	O(2)–Mo(2)–N(35)	93.2(3)	O(3)–Mo(3)–N(95)	93.6(4)
O(105)–Mo(1)–N(45)	87.8(3)	O(101)–Mo(2)–N(35)	166.6(3)	O(103)–Mo(3)–N(95)	88.0(3)
O(1)–Mo(1)–N(65)	91.8(4)	O(2)–Mo(2)–N(15)	94.4(4)	O(3)–Mo(3)–N(75)	90.3(4)
O(105)–Mo(1)–N(65)	163.8(3)	O(101)–Mo(2)–N(15)	90.3(3)	O(103)–Mo(3)–N(75)	165.2(4)
N(45)–Mo(1)–N(65)	85.2(3)	N(35)–Mo(2)–N(15)	83.5(3)	N(95)–Mo(3)–N(75)	85.4(3)
O(1)–Mo(1)–N(55)	168.7(4)	O(2)–Mo(2)–Cl(2)	98.5(3)	O(3)–Mo(3)–Cl(3)	99.3(3)
O(105)–Mo(1)–N(55)	85.9(3)	O(101)–Mo(2)–Cl(2)	92.3(2)	O(103)–Mo(3)–Cl(3)	92.1(3)
N(45)–Mo(1)–N(55)	79.8(3)	N(35)–Mo(2)–Cl(2)	91.1(3)	N(95)–Mo(3)–Cl(3)	166.6(3)
N(65)–Mo(1)–N(55)	78.6(3)	N(15)–Mo(2)–Cl(2)	166.3(3)	N(75)–Mo(3)–Cl(3)	91.2(3)
O(1)–Mo(1)–Cl(1)	98.9(3)	O(2)–Mo(2)–N(25)	172.6(3)	O(3)–Mo(3)–N(85)	167.9(4)
O(105)–Mo(1)–Cl(1)	92.1(2)	O(101)–Mo(2)–N(25)	84.2(3)	O(103)–Mo(3)–N(85)	86.3(3)
N(45)–Mo(1)–Cl(1)	167.2(3)	N(35)–Mo(2)–N(25)	82.9(3)	N(95)–Mo(3)–N(85)	79.2(4)
N(65)–Mo(1)–Cl(1)	91.5(2)	N(15)–Mo(2)–N(25)	78.9(3)	N(75)–Mo(3)–N(85)	79.4(4)
N(55)–Mo(1)–Cl(1)	87.4(2)	Cl(2)–Mo(2)–N(25)	88.0(3)	Cl(3)–Mo(3)–N(85)	87.4(3)
C(105)–O(105)–Mo(1)	139.0(7)	C(101)–O(101)–Mo(2)	139.7(7)	C(103)–O(103)–Mo(3)	137.7(7)

**Table 4.** Fractional Atomic Coordinates ( $\times 10^4$ ) and Equivalent Isotropic Displacement Parameters ( $\text{Å}^2 \times 10^3$ ) for **9**·5CH<sub>2</sub>Cl<sub>2</sub> (Solvent Molecules Omitted)

	<i>x</i>	<i>y</i>	<i>z</i>	<i>U</i> (eq)		<i>x</i>	<i>y</i>	<i>z</i>	<i>U</i> (eq)
Mo(1)	6182(1)	1229(1)	6257(1)	28(1)	C(57)	7604(10)	1501(3)	8473(10)	51(4)
Cl(1)	7269(2)	856(1)	7000(2)	46(1)	N(61)	4024(6)	1095(2)	6875(6)	28(2)
O(1)	6158(6)	1074(2)	5132(6)	40(2)	C(62)	3262(9)	886(3)	6809(9)	37(3)
B(1)	12085(10)	3068(3)	7083(11)	34(3)	C(63)	3624(9)	592(3)	6496(9)	44(3)
N(11)	12079(6)	2893(2)	6120(7)	29(2)	C(64)	4630(9)	634(3)	6352(9)	38(3)
C(12)	12745(9)	2887(3)	5471(8)	38(3)	N(65)	4875(7)	943(2)	6599(7)	29(2)
C(13)	12418(11)	2693(3)	4740(9)	50(4)	C(66)	2201(9)	970(3)	7053(11)	55(4)
C(14)	11501(9)	2572(3)	4997(8)	32(3)	C(67)	5337(9)	393(3)	6051(11)	48(4)
N(15)	11307(7)	2691(2)	5846(7)	32(2)	Mo(3)	10165(1)	858(1)	4097(1)	39(1)
C(16)	13704(9)	3089(4)	5563(10)	61(4)	Cl(3)	9891(3)	1300(1)	3121(3)	72(1)
C(17)	10774(12)	2354(3)	4473(10)	58(4)	O(3)	8979(6)	715(2)	4102(6)	45(2)
N(21)	12104(7)	2811(2)	7832(6)	27(2)	B(3)	12039(10)	355(3)	3729(10)	34(3)
C(22)	12754(8)	2763(3)	8569(8)	30(3)	N(71)	11267(7)	349(2)	2887(7)	35(2)
C(23)	12514(10)	2485(3)	9023(10)	43(3)	C(72)	11214(10)	169(3)	2113(10)	43(3)
C(24)	11676(9)	2366(3)	8516(8)	33(3)	C(73)	10337(10)	249(3)	1616(9)	47(4)
N(25)	11408(7)	2560(2)	7802(7)	29(2)	C(74)	9887(10)	485(3)	2112(9)	46(3)
C(26)	13571(9)	3010(3)	8820(10)	50(4)	N(75)	10455(7)	549(2)	2897(7)	35(2)
C(27)	11103(10)	2063(3)	8700(10)	48(3)	C(76)	11987(11)	-69(3)	1891(10)	55(4)
N(31)	11114(7)	3261(2)	7104(7)	32(2)	C(77)	8915(11)	656(4)	1876(12)	74(5)
C(32)	10980(10)	3580(3)	7191(9)	40(3)	N(81)	12490(7)	692(2)	3827(7)	39(3)
C(33)	9965(10)	3638(3)	7195(9)	45(3)	C(82)	13441(9)	796(3)	3852(9)	39(3)
C(34)	9507(9)	3341(3)	7088(8)	36(3)	C(83)	13427(11)	1119(3)	4025(10)	50(4)
N(35)	10206(7)	3102(2)	7044(7)	31(2)	C(84)	12441(10)	1215(3)	4112(10)	46(3)
C(36)	11826(11)	3819(3)	7298(13)	70(5)	N(85)	11867(8)	946(2)	3977(8)	44(3)
C(37)	8402(9)	3269(3)	7033(11)	52(4)	C(86)	14312(10)	575(4)	3684(13)	68(5)
Mo(2)	10071(1)	2597(1)	6740(1)	37(1)	C(87)	12039(13)	1539(3)	4234(14)	89(7)
Cl(2)	9059(3)	2527(1)	7953(3)	58(1)	N(91)	11547(7)	273(2)	4640(7)	28(2)
O(2)	9136(6)	2659(2)	5833(5)	30(2)	C(92)	11753(9)	47(3)	5292(9)	39(3)
B(2)	4076(10)	1435(3)	7217(10)	32(3)	C(93)	11113(9)	85(3)	6010(9)	37(3)
N(41)	4316(7)	1664(2)	6429(6)	27(2)	C(94)	10517(9)	353(3)	5760(9)	37(3)
C(42)	3849(9)	1927(3)	6089(9)	37(3)	N(95)	10778(7)	469(2)	4941(7)	32(2)
C(43)	4333(9)	2035(3)	5331(9)	40(3)	C(96)	12569(9)	-190(3)	5219(9)	43(3)
C(44)	5106(9)	1827(3)	5213(8)	31(3)	C(97)	9724(9)	499(3)	6301(9)	39(3)
N(45)	5115(7)	1602(2)	5887(7)	30(2)	O(101)	10261(5)	2139(2)	6599(6)	33(2)
C(46)	2974(10)	2075(3)	6553(10)	56(4)	C(101)	9742(8)	1877(2)	6335(8)	28(3)
C(47)	5863(9)	1831(3)	4491(8)	38(3)	C(102)	10237(8)	1628(3)	5938(8)	29(3)
N(51)	4928(7)	1467(2)	7980(6)	26(2)	O(103)	10280(6)	1125(2)	5195(6)	36(2)
C(52)	4912(11)	1576(3)	8893(8)	42(3)	C(103)	9743(8)	1366(2)	5596(8)	29(3)
C(53)	5908(11)	1609(3)	9202(9)	47(3)	C(104)	8708(8)	1334(3)	5678(8)	30(3)
C(54)	6478(9)	1508(3)	8492(9)	35(3)	O(105)	7206(5)	1552(2)	6245(6)	34(2)
N(55)	5877(7)	1423(2)	7733(7)	32(2)	C(105)	8217(8)	1573(3)	6111(8)	29(3)
C(56)	3986(10)	1647(3)	9357(9)	54(4)	C(106)	8699(8)	1846(3)	6450(8)	30(3)

droxybenzene (phloroglucinol). The 1,3,5-benzenetriyl unit has been exploited to give ferromagnetic exchange between three radical centers in organic molecules;<sup>33</sup> given the ferromagnetic exchange across the *meta*-substituted bridge of **2**, we reasoned that the trinuclear complex **9** should also be ferromagnetic with

an  $S = 3/2$  ground state since each pair of metals has a *meta* relationship across the bridge.

Complex **9** was prepared by the same route used for **1–4**,<sup>18</sup> and its crystal structure is in Figure 1 (see Tables 1, 3, and 4). There is no imposed symmetry in the complex; all three metal

centers are independent. Bond distances and angles around each metal center are typical of oxo-molybdenum(V) complexes (Table 3). The metal-metal separations are Mo(1)–Mo(2), 7.736 Å; Mo(2)–Mo(3), 8.172 Å; Mo(1)–Mo(3), 6.517 Å: it is likely that in solution rotational flexibility about the Mo–O(phenol) and O(phenol)–C bonds will average these.<sup>18</sup>

Electrochemical studies on **9** in CH<sub>2</sub>Cl<sub>2</sub> showed three reductions at  $E_{1/2} = -1.23$ ,  $-1.45$ , and  $-1.81$  V *vs* the ferrocene/ferrocenium couple (Fc/Fc<sup>+</sup>). The waves had equal anodic and cathodic peak currents, but the peak-peak separations  $\Delta E_p$  were in each case *ca.* 200 mV at a scan rate of 0.2 V s<sup>-1</sup>, which resulted in rather poor resolution in the cyclic voltammogram. The peak potentials could however be extracted readily from a square-wave voltammogram. The  $\Delta E_p$  values are much larger than would be expected for thermodynamically reversible one-electron processes and are larger than those observed for dinuclear complexes **1–4** under the same conditions.<sup>18</sup> This suggests kinetically slow electron-transfer, which may be related to the unusual proximity of the metal centers; using slower scan rates did not significantly decrease the  $\Delta E_p$  values, however their accurate measurement was not possible due to the proximity of the three waves in the cyclic voltammogram.

These processes are all metal-centered Mo(V)/Mo(IV) couples, and the separations between them indicate substantial electronic interactions between the three metal centers. This is in agreement with the properties of the related dinuclear complexes;<sup>18</sup> in particular, complex **2** has a separation of 200 mV between the Mo(V)/Mo(IV) couples across its *meta*-substituted bridge, which is similar to the separation of 220 mV between the first two reductions of **9**. The separation between the second and third reduction processes of **9** is substantially larger at 360 mV, because the third electron will be experiencing two unfavorable electrostatic interactions with the negative charges at the other two apices of the triangle. On purely electrostatic grounds therefore the separation between the second and third reductions should be approximately double the separation between the first and second reductions, which is indeed the case. The cyclic voltammogram also shows a single irreversible oxidation wave at +0.49 V *vs* Fc/Fc<sup>+</sup>, which we believe—again by analogy with the dinuclear complexes—to be largely centered on the bridging ligand. Complexes of *para*-substituted bridging ligands such as **1** and **3** have two reversible oxidations resulting in a species in which the bridging ligand has some quinone character; complex **2**, in which this is not possible due to the *meta* substitution pattern, has a single irreversible oxidation (like **9**).

The presence of ferromagnetic coupling within **9** was confirmed by a variable-temperature magnetic susceptibility study down to 1.2 K (Figure 2), which yielded  $J = 14.4$  cm<sup>-1</sup>. This is substantially larger than the  $J$  values for ferromagnetically-coupled complexes of first-row metal ions which have similar metal-metal separations across *meta*-substituted aromatic bridges.<sup>13–15</sup> This may be because the 4d orbitals of Mo have better spatial overlap with the  $\pi$ -orbitals of the bridging ligand than do the 3d orbitals of the first-row metals. Another significant factor will be sp<sup>2</sup> hybridization of the phenolate oxygen atoms, with the p<sub>z</sub> orbitals participating in conjugation between the metal centers and the central aromatic ring. The angles at the phenolate oxygen atoms are all between 137 and 139°, due to the steric crowding arising from having three bulky metal fragments close together. We note also that the exchange interaction in **9** is comparable in size (but opposite in sign)

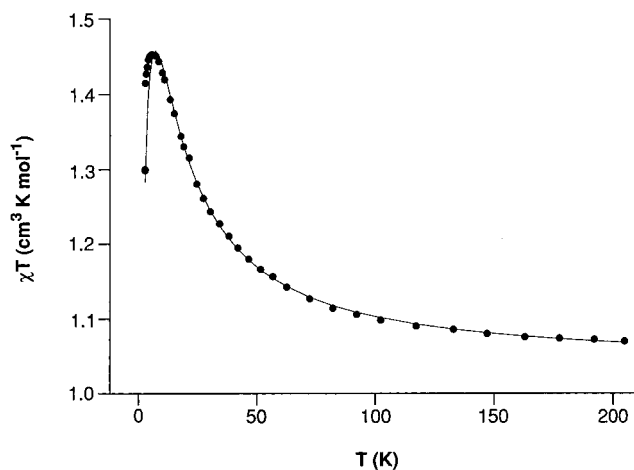


**Figure 2.** Temperature dependence of  $\chi T$  for complex **9** showing the experimental measurements (circles) and computed best-fit (solid line).

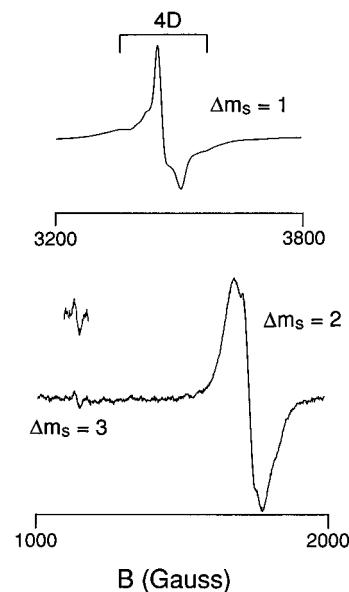


**Figure 3.** EPR spectrum of **9** as a frozen glass (CH<sub>2</sub>Cl<sub>2</sub>/thf, 1:1) at 77 K, showing (a) the  $\Delta m_s = 1$  transition and (b) the “forbidden”  $\Delta m_s = 2$  and  $\Delta m_s = 3$  transitions.

to those in trinuclear oxo-centered carboxylate clusters of Mn(III) and Fe(III) in which the metal ions are much closer together.<sup>34</sup>

The solution X-band EPR spectrum at room temperature shows a broad, featureless, symmetric signal ( $g_{\text{iso}} = 1.938$ , peak-peak separation 69 G). The absence of hyperfine structure is consistent with strong magnetic-dipole coupling between the unpaired electrons.<sup>35</sup> In trinuclear molybdenum complexes where the paramagnetic metal centers are more remote and therefore more weakly coupled, the expected set of hyperfine signals for coupling to three equivalent molybdenum nuclei is generally clearly apparent.<sup>23b</sup> The spectrum recorded at 77 K, as a frozen CH<sub>2</sub>Cl<sub>2</sub>/thf glass, is shown in Figure 3. The most important feature of the spectrum is that it shows  $\Delta m_s = 1$ , 2, and 3 transitions centered at 3473, 1739, and 1154 G, respectively ( $g = 1.94$ , 3.88, and 5.62); i.e., the  $\Delta m_s = 2$  and 3 transitions occur at almost exactly one-half and one-third, respec-

(33) Kanno, F.; Inoue, K.; Koga, N.; Iwamura, H. *J. Phys. Chem.* **1993**, *97*, 13267.

(34) (a) Vincent, J. B.; Chang, H.-R.; Foltling, K.; Huffman, J. C.; Christou, G.; Hendrickson, D. N. *J. Am. Chem. Soc.* **1987**, *109*, 5703. (b) Cannon, R. D.; Jayasooriya, U. A.; Wu, R.; arapKoske, A. K.; Stride, J. A.; Nielsen, O. F.; White, R. P.; Kearley, G. J.; Summerfield, D. *J. Am. Chem. Soc.* **1994**, *116*, 11869.

(35) Kothe, G.; Ohmes, E.; Brickmann, J.; Zimmermann, H. *Angew. Chem., Int. Ed. Engl.* **1971**, *10*, 938.

tively, of the field of the major  $\Delta m_s = 1$  transition. The relative intensities of the three transitions are  $1:4 \times 10^{-4}:8 \times 10^{-7}$ . Observation of  $\Delta m_s = 3$  transitions in quartet species is rare due to their extremely low intensity. They have mostly been observed in organic triradicals,<sup>36,37</sup> although there are examples for triangular trinuclear complexes of Cu(II)<sup>38</sup> and Ti(III).<sup>15a</sup>

The  $\Delta m_s = 1$  transition of a randomly-oriented quartet species with 3-fold symmetry should have five equally-spaced lines of which the central one should be much stronger than the others,<sup>39</sup> the separation between the lines being the zero-field splitting parameter  $D$ . Spectra of this type are well-known in organic triradicals.<sup>36,40</sup> The  $\Delta m_s = 1$  transition of **9** conforms approximately to this (Figure 3) although departures from ideality may be ascribed to the presence of orbital angular momentum (which is quenched in organic polyradicals)<sup>41</sup> giving an anisotropic  $g$ -tensor, and/or the possible absence of strict 3-fold symmetry, in particular a rhombic component. The separation between the outermost lines is  $4D$ , giving  $D = 50$  G ( $0.0046 \text{ cm}^{-1}$ ). The  $\Delta m_s = 2$  transition should consist of four lines at  $0.5H_0 \pm 0.5D$  and  $0.5H_0 \pm D$ ;<sup>39</sup> these are not clearly resolved, but some structure is apparent on the signal. The  $\Delta m_s = 3$  transition should be a single line<sup>39</sup> and appears to be so.

- (36) (a) Weissman, S. I.; Kothe, G. *J. Am. Chem. Soc.* **1975**, *97*, 2537. (b) Rajca, A.; Utamapanya, S. *J. Am. Chem. Soc.* **1993**, *115*, 2396. (c) Müller, U.; Baumgarten, M. *J. Am. Chem. Soc.* **1995**, *117*, 5840.
- (37) Ozarowski, A.; McGarvey, B. R.; El-Hadad, A.; Tian, Z.; Tuck, D. G.; Krovich, D. J.; DeFotis, G. C. *Inorg. Chem.* **1993**, *32*, 841.
- (38) (a) Siedle, A. R.; Padula, F.; Baranowski, J.; Goldstein, C.; De Angelo, M.; Kokoszka, G. F.; Azevedo, L.; Venturini, E. L. *J. Am. Chem. Soc.* **1983**, *105*, 7447. (b) Kokoszka, G. F.; Padula, F.; Goldstein, C.; Venturini, E. L.; Azevedo, L.; Siedle, A. R. *Inorg. Chem.* **1988**, *27*, 59.
- (39) Brickmann, J.; Kothe, G. *J. Chem. Phys.* **1973**, *59*, 2807.
- (40) (a) Yoshizawa, K.; Chano, A.; Ito, A.; Tanaka, K.; Yamabe, T.; Fujita, H.; Yamauchi, J.; Shiro, M. *J. Am. Chem. Soc.* **1992**, *114*, 5994. (b) Stickley, K. R.; Blackstock, S. C. *J. Am. Chem. Soc.* **1994**, *116*, 11576.
- (41) Slichter, C. P. *Principles of Magnetic Resonance*; Harper & Row: New York, 1963; Chapters 4 and 7.

Overall the EPR spectrum confirms the quartet nature of the ground state which was apparent from the susceptibility measurements.

## Conclusions

We have shown that in two series of complexes containing two or three paramagnetic molybdenum fragments attached to aromatic bridging ligands the exchange interaction between the metal termini is dependent on both the topology of the bridging ligand (*para*-substituted bridging ligands give antiferromagnetic coupling whereas *meta*-substituted bridges give ferromagnetic coupling) and the conformation of the bridging ligand (the magnitude of  $J$  is substantially diminished by introducing sterically a twist between two aromatic rings in the bridging pathway). All of the results are consistent with the exchange interactions being transmitted *via* the  $\pi$ -electrons of the bridging ligand by a spin-polarization mechanism, which is facilitated by good overlap between the magnetic  $d(\pi)$  orbitals of the metal centers and the  $\pi$ -orbitals of the bridging ligands. The strength of the interactions compared to related complexes with first-row metal ions is ascribed to the better overlap of 4d metal orbitals compared to 3d orbitals with the bridging ligand. The significance of these results is 2-fold: (i) The sign of a magnetic interaction between metal centers can be predetermined by a suitable choice of bridging ligand; (ii) steric (or allosteric) control of the conformation of the bridge is a possible switching mechanism in magnetic materials based on coordination polymers.

**Acknowledgment.** We thank the EPSRC (U.K.) for a Ph.D studentship (to V.A.U.) and a post-doctoral fellowship (to A.M.W. C.T.), and for grants to purchase the diffractometer and EPR spectrometer. We also thank Dr. J. P. Maher for assistance with recording the EPR spectra of **9**.

IC9610086